



# Seismological observations in Northwestern South America: Evidence for two subduction segments, contrasting crustal thicknesses and upper mantle flow



Jefferson Yarce <sup>a,\*</sup>, Gaspar Monsalve <sup>a</sup>, Thorsten W. Becker <sup>b</sup>, Agustín Cardona <sup>a</sup>, Esteban Poveda <sup>c</sup>, Daniel Alvira <sup>a</sup>, Oswaldo Ordoñez-Carmona <sup>a</sup>

<sup>a</sup> Universidad Nacional de Colombia, Medellín Campus, Colombia

<sup>b</sup> University of Southern California, United States

<sup>c</sup> Federal University of Rio Grande do Norte, Brazil

## ARTICLE INFO

### Article history:

Received 24 June 2014

Received in revised form 17 September 2014

Accepted 21 September 2014

Available online 2 October 2014

### Keywords:

Colombian Andes

Caribbean slab

Nazca slab

Teleseismic travel time residuals

Pn-wave speed

## ABSTRACT

The cause of tectonic deformation in northwestern South America and its link to upper mantle structure and flow are debated. We use a combination of broadband and short period travel time seismic data for P-waves to show that observations are consistent with the presence of two subduction segments in Colombia and contrasting values of crustal thickness. In Northern Colombia, at latitudes greater than 6°N, most of the seismic stations are associated with negative teleseismic travel time residuals, relative to a regional mean, suggesting that the upper mantle is seismically faster than predicted from global models. In particular, for the Caribbean coastal plains there are no signs of significant anomalies in the upper mantle, evidenced by the small magnitude of the travel time delays and subdued Pn speeds (~7.97 km/s). To the southeast of such plains there is an increase in magnitude of the negative travel time residuals, including the Northern Eastern Cordillera, the Perija Range and the Merida Andes. An analysis of non-isostatic residual topography, based on a model of crustal thickness in northwestern South America, is consistent with a slab-associated upper mantle flow beneath the region just east of the Bucaramanga Nest. We interpret these results to indicate the presence of a Caribbean slab, initially flat beneath the Caribbean coastal plains, and steepening sharply in the southeast, including the area of Bucaramanga. For most of the western Andean region and the Pacific coast, south of 6°N, teleseismic differential travel time residuals are predominantly positive, indicating that the upper mantle is in general seismically slower than the reference model. Beneath the Central Cordillera, just to the east of this area, the residuals become smaller and predominantly negative; residual non-isostatic topography is negative as well. These features are probably related to the effect of the Nazca subduction developing an asthenospheric wedge.

© 2014 Elsevier B.V. All rights reserved.

## 1. Introduction

A range of previous studies have focused on the tectonic setting, boundaries and characteristics of the Nazca and Caribbean plate segments subducting under the North Andean block (Fig. 1). Seismicity and tomographic images have been used for this purpose. Pennington (1981) proposes the presence of two subduction segments in the northwesternmost Andes (Bucaramanga and Cauca). Van der Hilst and Mann (1994) suggest the existence of the Maracaibo (Caribbean related) and Bucaramanga (Nazca related) slabs beneath the North Andean Block. Taboada et al. (2000) and Cortes and Angelier (2005) proposed an association between the Bucaramanga Seismic Nest (Fig. 1) and Caribbean subduction. Gutscher et al. (2000) presented a model of flat subduction beneath Northwestern Colombia related to

the Panama–Choco Block collision, which steepens at the location of the Bucaramanga nest. Hypocentral relocations by Ojeda and Havskov (2001) also suggest the existence of two segments, but their association with subducted slabs is still unclear.

There are still open questions about the spatial extent of the subducted Nazca and Caribbean slabs beneath Colombia and their possible interaction in depth. Pennington (1981) proposes the existence of a WNW-ESE oriented shear zone in the contact area between both plates, but other authors consider that there is a region where they overlap. Shih et al. (1991) use results of attenuation of seismic waves, in particular a region of low attenuation, as evidence for overlapping slabs. Van der Hilst and Mann (1994) and Corredor (2003) correlate this possible overlapping zone with the absence of volcanism in the Andean region north of 5.5°N. Taboada et al. (2000) suggest that the interaction between slabs originates active faulting within both. According to the models of Cortes and Angelier (2005) there is a region in northern Colombia where both slabs overlap, with the Caribbean

\* Corresponding author. Tel.: +57 3104493651 (mobile).  
E-mail address: [jjarce@unal.edu.co](mailto:jjarce@unal.edu.co) (J. Yarce).

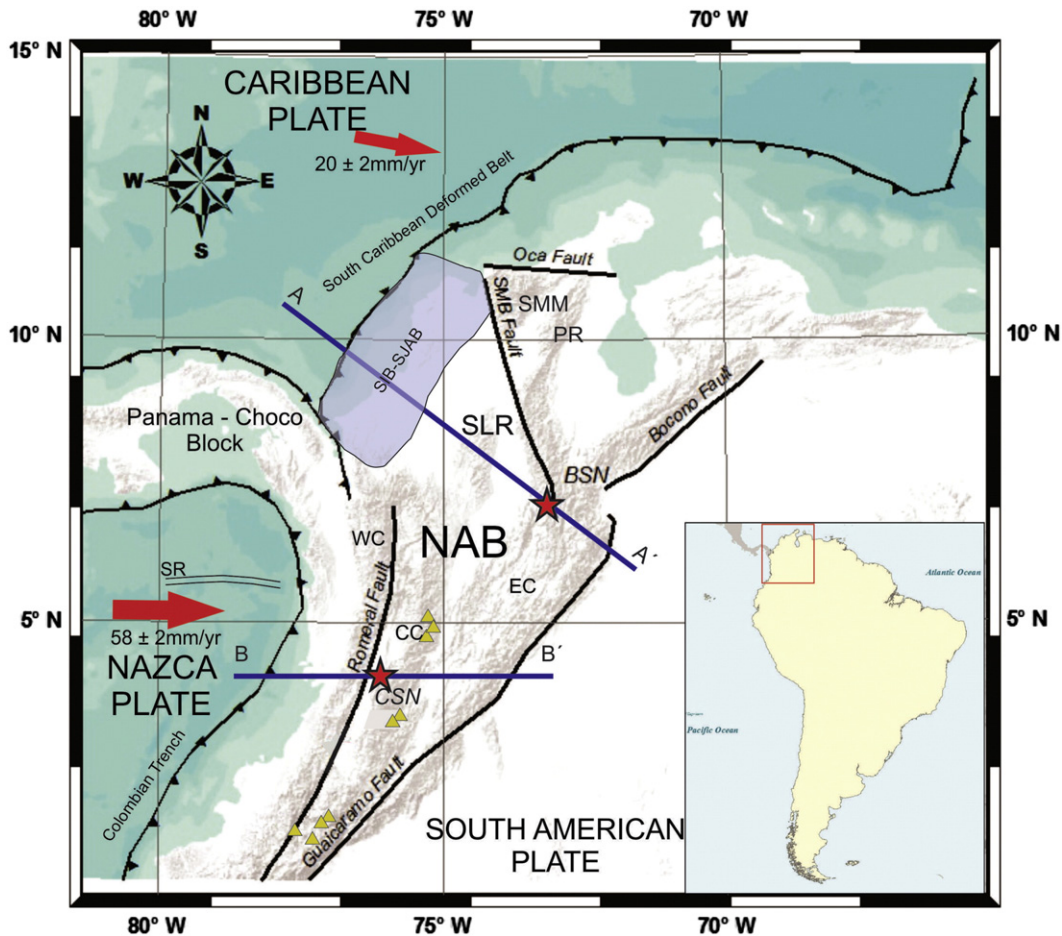


**Fig. 1.** Simplified tectonic map of Colombia with major fault systems: Romeral, Guacaramo, Santa Marta–Bucaramanga (SMB), Bocono and Oca Fault. Red stars indicate the location of seismic nests: Cauca Seismic Nest (CSN) and Bucaramanga Seismic Nest (BSN); main mountain ranges: Western Cordillera (WC), Central Cordillera (CC), Eastern Cordillera (EC). Red arrows indicate vectors of movement of each plate relative to stable South America. NAB (Trenkamp et al., 2002): North Andean Block, SR: Sandra Ridge; SMM: Santa Marta Massif, PR: Perija Range and SLR: San Lucas Range. SIB-SJAB: Sinu and San Jacinto Basins. Lines AA' and BB' correspond to schematic cross-sections shown in Fig. 10. Green triangles represent Volcanic complexes in Colombia.

plate on top of the Nazca plate, coinciding with a region of high seismicity; their idea of slab interactions includes a suggestion that the Bucaramanga and Cauca seismic nests (Fig. 1) are the result of tearing of Caribbean and Nazca slabs respectively. Vargas and Mann (2013) suggested a boundary between Nazca and Caribbean subductions represented by the “Caldas Tear”, a continental extension of the Sandra Ridge, with a nearly W-E trend at a latitude of  $\sim 5.5^\circ\text{N}$ .

Here, we use travel time data from teleseismic and regional earthquakes recorded at stations of the National Seismological Network of Colombia (*Red Sismológica Nacional de Colombia, RSNC*). Particularly, we looked at travel time residuals of teleseismic events to separate regions of seismically slow and fast upper mantle, and travel times of regional events to constrain the spatial variations in the uppermost mantle P-wave speed. This approach was used to identify regions of contrasting upper mantle temperatures and crustal thicknesses, related to the complex subduction system beneath the Northern Andes.

## 2. Geodynamic setting

The Andes of Colombia are located in a tectonically complex region where at least three tectonic plates converge. Much of the deformation resulting from these interactions is absorbed in the Panama–Choco and the North Andean Blocks (Cortes and Angelier, 2005; Kellogg and Vega, 1995; Pennington, 1981). The latter include the Colombian orogenic system, composed of three cordilleras (Western, Central and Eastern Cordilleras [Fig. 1]).

According to Trenkamp et al. (2002) the Nazca Plate is moving in a nearly eastward direction with a convergence rate of  $58 \pm 2$  mm/yr, and the Caribbean Plate moves in an ESE direction with a rate of convergence of  $20 \pm 2$  mm/yr, both relative to stable South America. The North Andean Block, which includes the volcanic arc and the three main cordilleras, moves in NE direction with respect to the South American Plate at an approximate speed of 6 mm/yr. Volcanic activity in this block started in the Cretaceous (Marriner and Millward, 1984) and continued through the Cenozoic until it reached its present configuration (at least a million years ago (Calvache et al., 1997)) and is located  $\sim 250$  km from the Nazca trench.

According to Pennington (1981), the Nazca Plate subducts beneath south western Colombia (the North Andean Block) with an angle of nearly  $35^\circ$  in a NW-SE direction, defining what he calls the Cauca Segment, which includes the Cauca seismic nest (also called Viejo Caldas seismic nest (Franco, 2002)) (Fig. 1), whereas the Caribbean Plate subducts beneath the North Andean Block at a shallower dip in a WNW-ESE direction, defining the Bucaramanga Segment, and including the Bucaramanga Seismic Nest (Fig. 1).

The formation of the Nazca plate took place after the fragmentation of the Farallon plate during the Late Oligocene–Early Miocene (Hoernle et al., 2002; Lonsdale, 2005; Meschede and Barchhausen, 2000). The Nazca plate, in the vicinity of the subduction zone beneath Colombia, seems to be relatively young: over the last 20 m.y. several events of sea floor spreading have been reported in this plate, which means very young ages of the lithosphere distributed in an asymmetric pattern

(Müller et al., 2008). Between latitudes 2° and 6°N, Tibaldi and Ferrari (1992) report ages for the Nazca Plate between 2 and 16 m.y. The Caribbean Plate originated in the Cretaceous as an oceanic plateau within the Pacific, and moved first in a north direction and then ENE, until reaching its current location (Kennan and Pindell, 2009; Kerr and Tarney, 2005).

### 3. Data and methods

Seismological catalog data in Colombia are available from the RSNC, operated by the Colombian Geological Survey, since 1993; however, it was not until 2008 that broadband stations began to be systematically installed all over the country. Combined with the short period pre-existing stations, this allows us to have a set of reliable arrival times from near and distant earthquakes. The recording stations are shown in Fig. 2.

Travel time residuals are the differences between observed and calculated travel times of a seismic ray that goes from a source to a receiver. The calculated time can be obtained by using a reference Earth model, which in our case is *iasp91* (Kennett and Engdahl, 1991), and was computed using the *TauP* software (Crotwell et al., 1999). When using teleseismic events, absolute travel time residuals are mainly due to both near-source and near-receiver effects, which represent anomalies in the crust and/or the upper mantle. The use of relative (or differential) travel time residuals of global events recorded at a local/regional network allows us to isolate the effects of near-receiver structure (e.g. Ding and Grand, 1994; Zhou et al., 1996). Here, we used events recorded at several stations, and calculated the difference in time residuals among all the possible station pairs. We then collected the mean differential residual at all stations relative to each one of the others, and calculate an average of them. This allows us to estimate

an average regional residual and to express the other residuals (time delays) relative to it.

In order to be able to deduce the presence of seismic anomalies in the upper mantle beneath North Western Colombia, we used teleseismic events from January 2008 to August 2012, with a minimum local magnitude of 5.5 and epicentral distances between 30° and 90°, recorded at stations of the RSNC, and calculated absolute and relative travel time residuals. The events used and their azimuthal coverage are illustrated in Fig. 3. Events with magnitudes over 6.5 have an associated P-arrival picking accuracy above 0.2 s, whereas earthquakes of smaller magnitude could have an arrival time uncertainty of up to 0.4 s (see supplemental material for some example seismograms).

If we want to identify the effects of the upper mantle structure in the travel time residuals, we need to take into account the crustal thickness variations, and take out from the differential time residual the portion that is due to the difference in crustal thickness between stations. For crustal thickness beneath the recording stations we used the global model CRUST 1.0 (Laske et al., 2013), combined with regional crustal thickness compilations by Assumpção et al. (2013), and recent receiver function estimates by Monsalve et al. (2013) and Poveda et al. (under review). These studies indicate very contrasting values of crustal thickness in the North Western Andean region, with thicknesses below 30 km in the Pacific and Caribbean coastal plains, and values of nearly 60 km beneath some of the Andean volcanoes of South Western Colombia and underneath the Eastern Cordillera in the Bogotá area. In the Northern Central Cordillera, high thicknesses have been reported, which exceed 50 km (Poveda et al., under review). The resulting, merged crustal thickness map is illustrated in Fig. 4. We took a reference crustal thickness of 39.8 km, and calculated the residual portion due to the difference in crustal thickness between any station and this reference value, using a mean crustal P-wave velocity estimated with the *iasp91* model. To find the differential travel time residuals corrected by crustal thickness variations beneath each station, we used the following equation:

$$Diff. Residual_c = Diff. Residual_0 - Diff. CrustalDelay \quad (1)$$

Where *Diff. Residual<sub>c</sub>* is the differential travel time residual after correction for crustal thickness, *Diff. Residual<sub>0</sub>* is the initial differential residual (before crustal correction) and *Diff. CrustalDelay* is a time that we calculated as follows:

$$Diff. CrustalDelay = \frac{\Delta Thickness}{Differential Velocity} \quad (2)$$

Where  $\Delta Thickness$  is defined as the difference between the thickness beneath each station and the regional average thickness (in this case 39.8 km); *Differential Velocity* is defined as follows:

$$Differential Velocity = \frac{1}{\frac{1}{V_c} - \frac{1}{V_m}} \quad (3)$$

Where  $V_c$  and  $V_m$  are the weighted averages of the crust and upper mantle velocities, respectively. The whole methodology for the relative travel time delay estimation is summarized in Fig. 5.

For a crude estimation of the P wave speed of the uppermost mantle in certain areas of northwestern Colombia, which can give us some clues about the upper mantle structure, we used the arrival times of regional earthquakes for which the first arrival corresponds to the P<sub>n</sub> phase. For this purpose, we used the catalog data from the RSNC, associated to events that occurred between January 1993 and August 2012, with a minimum local magnitude of 3.5. Given a mean crustal thickness in Colombia between 30 and 40 km (Ojeda and Havskov, 2001), regional events registered by the Colombian Seismological Network with crustal depths and epicentral distances above 170 km can be used for this

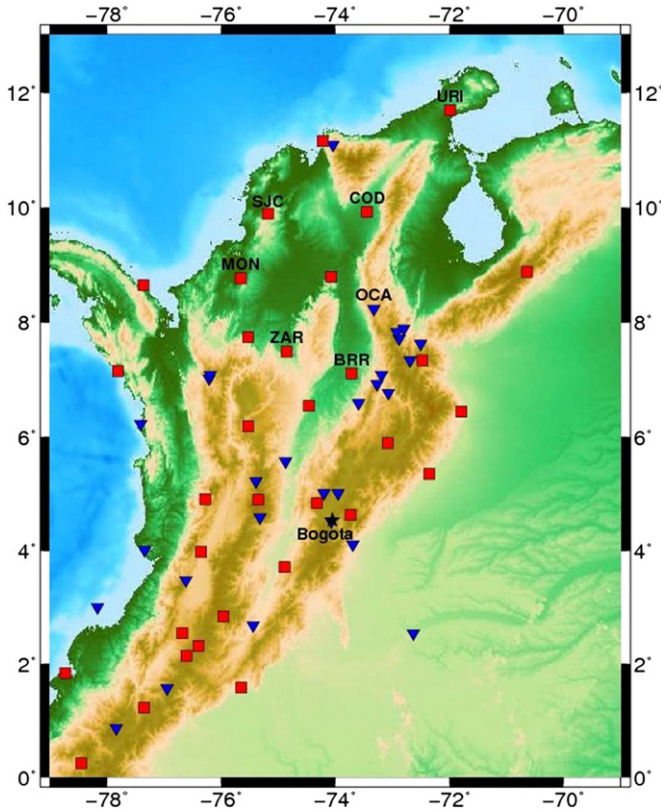


Fig. 2. Stations of the National Seismological Network of Colombia and neighboring regions used in this analysis. Red squares represent broadband stations, inverted blue triangles indicate short period – one component stations. Station codes are shown for locations mentioned in the discussion.

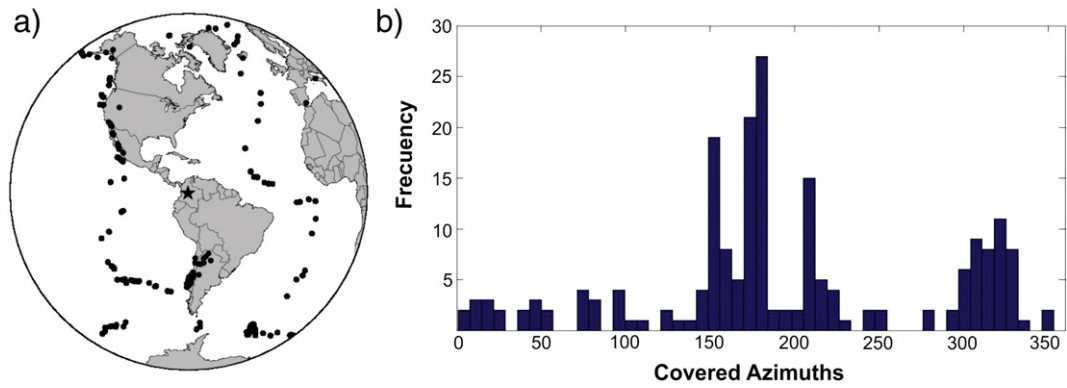


Fig. 3. a) Events used in this study (epicentral distances from 30° to 90°, with respect to Bogota) and b) azimuthal coverage, with respect to the city of Bogota, of events shown in a).

purpose (Fig. 6); this distance was chosen as an approximate upper limit for the cross-over distance in this region, so that at epicentral distances greater than this value, the first arrival is Pn. We used earthquakes whose location had an associated RMS of the time residuals below 1 s; for these events, the accuracy for the first arrival pick on the catalog was better than 0.15 s. Using a similar technique to the one explained in *Wéber (2002)* and *Monsalve et al. (2008)*, we combined information from different seismic events and multiple seismic stations, and looked at travel time versus epicentral distance

distributions in order to deduce the mean Pn velocities beneath several regions in Colombia, by estimating the slope of the time versus distance curve. We also made a sphericity correction in order to take into account the differences between distances traveled along the Moho and their projections at the earth surface. To be able to appreciate differences in the mean Pn speeds between various regions with morphotectonic and geodynamic significance, we grouped together stations in three areas: The Caribbean plains, the northern Eastern Cordillera, and a region north of 4°N in the

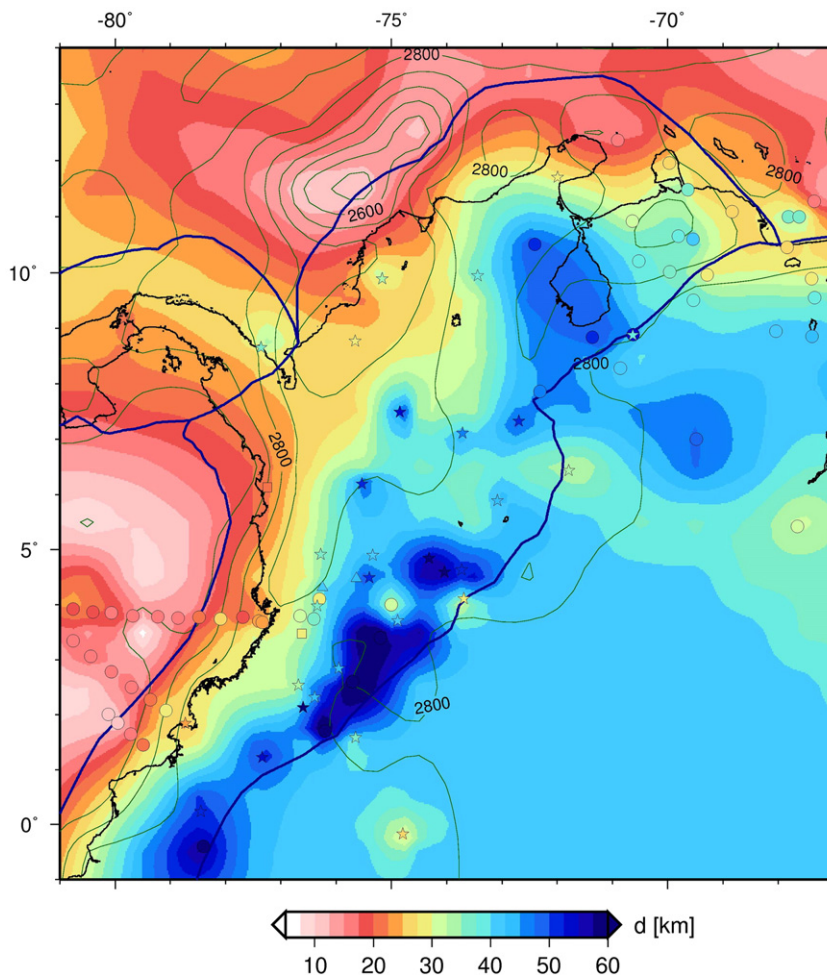


Fig. 4. Crustal thickness,  $d$ , model derived from merging the global,  $10 \times 10$  model CRUST1 (*Laské et al., 2013*) with the regional compilation from *Assumpção et al. (2013)* (circle symbols) and the receiver function estimates from *Monsalve et al. (2013)* (squares), and *Poveda et al. (under review)* (stars). Superimposed contours indicate crustal density (in  $50 \text{ kg/m}^3$  contour intervals) after converting the CRUST1 structure into average layer values. Plate boundaries (dark blue) are from *Bird (2003)*; most of Colombia is within the “Northern Andes” plate.

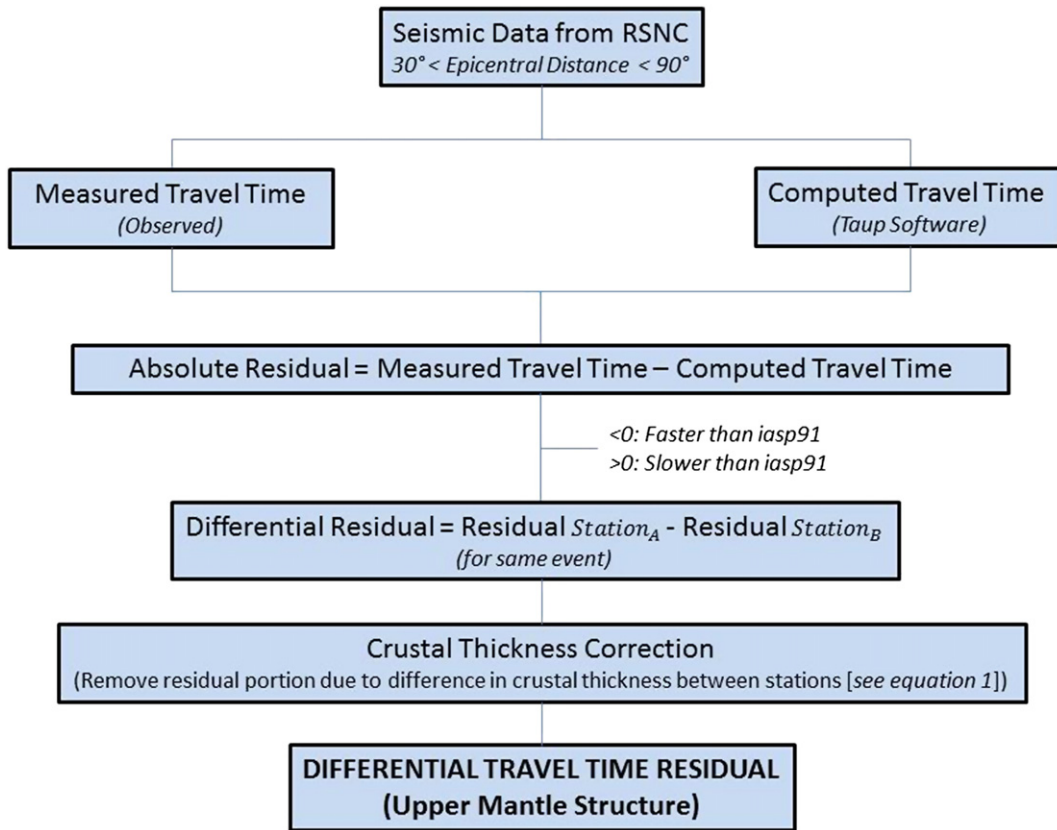


Fig. 5. Flow chart summarizing the whole methodology to obtain the differential travel time residuals corrected by crustal thickness variations between stations.

Cordilleran system, which includes the Western Cordillera, the Central Cordillera, and the Eastern Cordillera at latitudes below 5.5°N; these groups of stations are represented by purple, blue and red inverted triangles in Fig. 6, respectively.

#### 4. Results

In Fig. 7 we show the mean values of the estimated absolute travel time residuals at different stations in Colombia; the standard deviations are below 3 s, and we made sure that the number of data points per station was above 10 (see supplemental material for frequency histograms of absolute residuals at different stations). The average RMS of these mean absolute travel time residuals is 2.5 s. Negative residuals concentrate in the northern part of the study area, including the Caribbean coastal plains and the northern Eastern Cordillera. To the south of latitude ~6°N, the residual signal is more random, with a tendency to be positive. This suggests that seismic velocities in the crust and/or upper mantle for the northernmost part of Colombia are faster than they are in the reference model. In the south, that trend is reversed, indicating that seismic velocities are, in general, slower than in the reference model.

The calculated absolute travel time residuals are mainly a function of the near-source and near-receiver structure. The effects of the near-source structure should be minimal due to the variety of epicentral distances and back-azimuths of the events used (Fig. 3) (see supplemental material). Nevertheless, to further minimize such effect and focus on the near-receiver cause of those delays, we calculated the average differential travel time residuals at all stations relative to each one of the other receivers. This allows us to calculate a regional average for those delays, and therefore, to compute the time residuals relative to such regional mean. Those relative time delays are partially due to the difference in crustal thickness between stations. Since crustal thickness can have variations greater

than 20 km in the study area (Poveda et al., 2013, under review), we need to subtract from the differential residuals the effect in time delay of these differential thicknesses. Therefore, using the results of crustal thickness shown in Fig. 4, we corrected the relative average time residuals so that they best represent the differences in the upper mantle structure between station locations. For the estimation of time delays due to differences in crustal thickness we used a weighted average of crustal and uppermost mantle velocities given by the *iasp91* model (Kennett and Engdahl, 1991). The variability of the relative travel time residuals for all stations before and after crustal correction stays almost the same, with an RMS of 1.2 s. Uncertainties in Moho depth from receiver functions calculated by Poveda et al. (under review) are below  $\pm 4$  km, which may represent an uncertainty of around 0.16 s in the crustal travel time of the teleseismic rays. We normalized those relative time delays to a reference average crustal thickness of 39.8 km.

The results of differential travel time residuals, relative to a regional average, with the effect of differential crustal thickness subtracted from them, are illustrated in Fig. 8 where we still observe that negative residuals concentrate more in the north, and the positive ones are more predominant south of ~6°N; a significant difference in upper mantle structure must then exist between these two regions: a simple interpretation might suggest that the upper mantle is colder in the north than it is in the south. Stations near the Caribbean coast (MON, SJC, Fig. 2) have relatively small negative time residuals (Fig. 8), indicating that the coldest anomaly should concentrate to the south-east of the Caribbean coast, including the region of the Bucaramanga nest (Fig. 1), where time delays are strongly negative (Fig. 8). At the Pacific coast and the Western and Central Cordilleras, including the volcanic chain, there is a concentration of positive time delays (Fig. 8), and they become lower toward the east, beneath the intermountain Valley and the Eastern Cordillera, (Fig. 8).

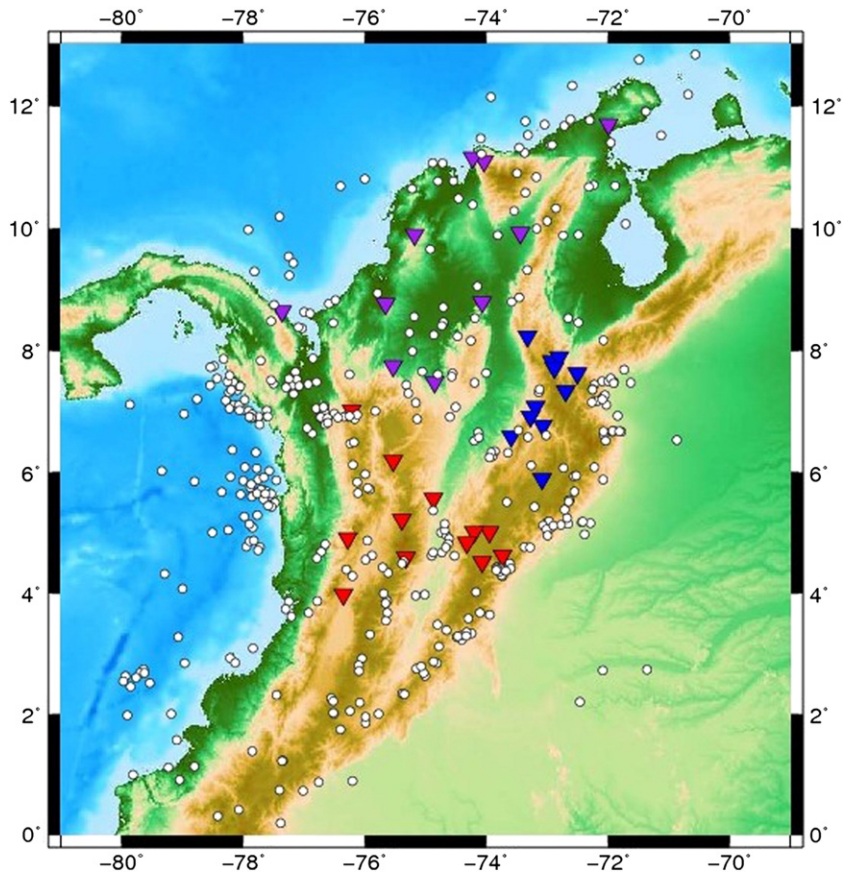


**Fig. 6.** Seismic events (white circles) and stations (inverted triangles) used for P-wave speed estimations. Purple, blue and red triangles represent stations used to estimate Pn speeds in the central Andean region, in northern Eastern Cordillera and in northernmost Colombia, respectively.

Slopes of travel time versus epicentral distance distributions suggest that Pn speeds have a mean value of  $7.97 \pm 0.05$  km/s for northernmost continental Colombia (calculated using arrival times at purple stations in Fig. 6),  $8.07 \pm 0.02$  km/s for the northern Eastern Cordillera (blue stations in Fig. 6), and  $8.05 \pm 0.03$  km/s for the Western Cordillera, the Central Cordillera and the Eastern Cordillera south of  $\sim 5^\circ\text{N}$  (red stations in Fig. 6). For these three regions, the number of used data points (Pn arrivals) was 173, 1190 and 686 respectively. The mean Pn values obtained for the three analyzed regions (Fig. 6) are within the typical values for Pn velocities in continental areas, although they are below the global average of 8.09 km/s (Christensen and Mooney, 1995). Pn speeds below 7.9 km/s are diagnostic of volcanic areas, magmatic activity, partial melt, water coming from subducted lithosphere, or a combination of one or several of those with a thin crust (e.g. Hearn and Ni, 1994; Hearn et al., 1994; Stern et al., 2010; Weber, 2002); values above around 8.15 km/s are typical of old, stable regions, cold upper mantle and relatively thick crust or lithosphere (Amini et al., 2012; Hearn and Ni, 1994; Hirn and Sapin, 1984; Lu et al., 2011), and in some cases they might be associated with continental collision (Hirn and Sapin, 1984; Monsalve et al., 2008). For the regions analyzed here, neither of those seems to be the case, and the obtained differences in Pn speeds are likely a consequence of crustal thickness variations. There is a difference of  $\sim 0.08$  km/s in the Pn speed below the Northern Colombia/Caribbean plains and the Andean region. The difference in crustal thickness between these two regions is between 15 and 30 km (Ceron et al., 2007; Poveda et al., 2013, under review), which should be enough to account for the observed contrast in Pn speed (Christensen and Mooney, 1995). Although the relative travel time residual suggests that there might be a difference in the thermal upper mantle structure between the Caribbean coastal

plains/Northern Eastern Cordillera and the rest of the Colombian Andes/Pacific coastal plains, the Pn results indicate that the sources of those differences are not at depths close to the Moho.

## 5. Discussion

The travel time residuals we measure indicate that there are important differences in the upper mantle structure between Northern Colombia and its Central and Western continental regions. The division is at  $\sim 6^\circ\text{N}$ , suggesting the presence of two subduction segments of different nature beneath Northwestern South America, one related to the Caribbean plate and the other associated with the Nazca plate.

The Caribbean Plate in the vicinities of the Colombian Coast consists mainly (but not exclusively) of an oceanic Cretaceous plateau (Mauffret and Leroy, 1997). According to Cloos (1993), a Cretaceous oceanic plateau should be negatively buoyant enough to subduct, and they are commonly associated with flat subduction (e.g. vanHunen et al., 2002). The presence of subduction in the Caribbean coastal plains of Colombia has been documented by Middle Miocene ( $\sim 13$ – $14$  ma) volcanism near station MON (Fig. 2) (Lara et al., 2013), and the current absence of volcanism near the coastline might indicate a present shallow Caribbean slab subduction. In this region it is highly possible that the Moho depicted in Fig. 4 corresponds to the crust-mantle boundary within the subducted oceanic plate. Relative time delays near the Caribbean coastline (stations MON, SJC, Fig. 2, see time delays in Fig. 8), which are relatively small, allow us to infer that there are no significant thermal anomalies in the upper mantle beneath this region, which is consistent with the absence of an asthenospheric wedge. Although the obtained mean Pn speed in this region is relatively small ( $\sim 7.97$  km/s), it must be due to the thin crust (Fig. 4) of continental

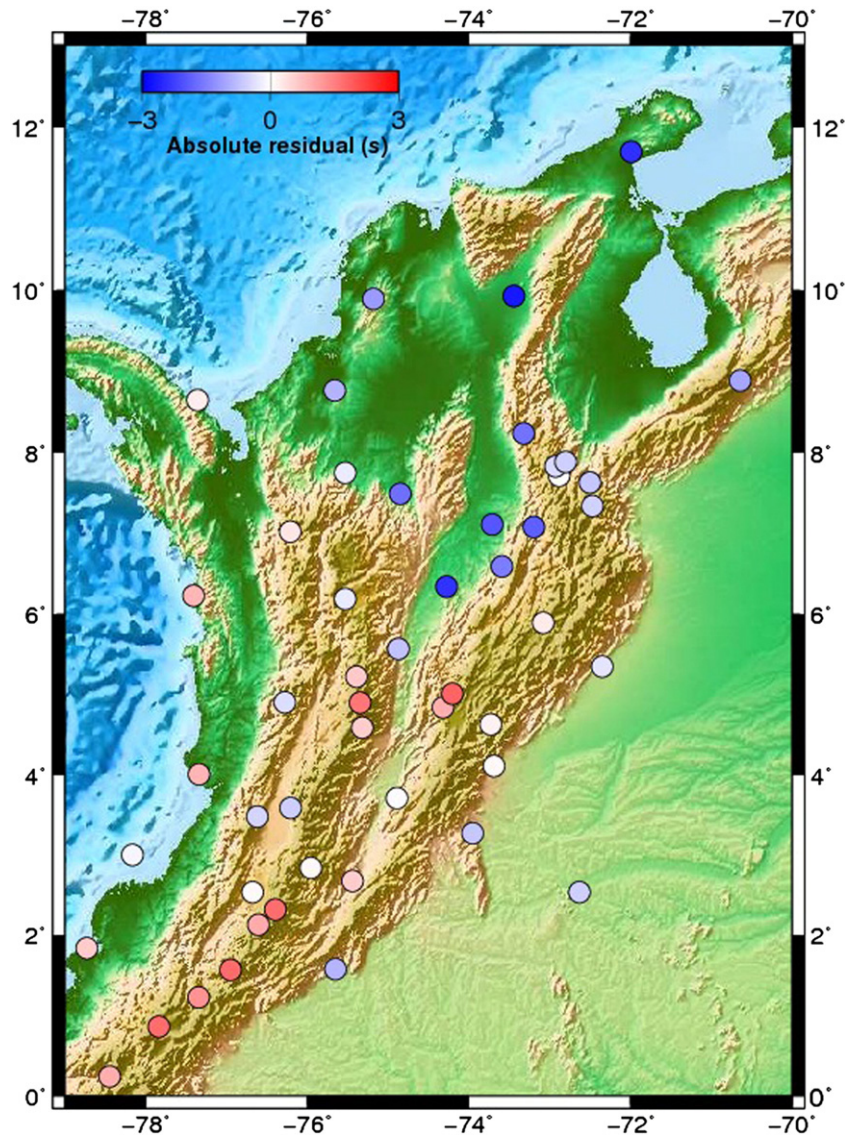


Fig. 7. Average, absolute teleseismic travel time residuals at each station. Note the concentration of negative travel time residuals to the north of the study region. See text for explanation.

nature (Maya, 1992) beneath the Caribbean Coastal plains, and there is no evidence for a hot uppermost mantle.

Even though northernmost Colombia has been a region associated with subduction under a continental margin at least from the middle Miocene (Lara et al., 2013), there is a current high oblique component in the convergence (Trenkamp et al., 2002). Although there are signs of a compressional regime at the Sinu-San Jacinto Basin, expressed by the presence of an accretionary wedge (Flinch, 2003; Toto and Kellogg, 1992), Cardona et al. (2012) hypothesize about various stages in the convergence process, which include an extensional episode of formation and filling of a post-collisional basin during the late Paleocene through the early Oligocene at the area of Sinu-San Jacinto (Fig. 1), and several changes in the obliquity of the convergence. Montes et al. (2010) presented evidence for as much as 115 km of extension to the south-west of the Santa Marta Massif during Oligocene through late Miocene time, probably linked to an oblique convergence and a clockwise rotation of this massif. To the NE of the Oca Fault Zone (Fig. 1), there is geological and geophysical evidence of extension during Tertiary times (Bonini, 1984), also documented by the stratigraphic record through the Eocene, Oligocene and Miocene (Macellari, 1995). These hypotheses are consistent with the seismological observations, which suggest a thin crust, with an absence of significant thermal anomalies in the uppermost mantle.

To the SE of the Caribbean coastline, in the vicinities and beneath the Perija Range, the San Lucas Range and the Northern Eastern Cordillera (Fig. 1), the relative time delays have a strong trend toward negative values (Fig. 8, stations ZAR, BRR, OCA, COD and neighboring sites in Fig. 2). At these locations, the upper mantle must be colder than beneath the northern coastal plains. A steepening of the Caribbean slab may occur around this area, and the cold upper mantle might be related with the slab penetrating the asthenosphere. In fact, subduction of the Caribbean Plate at a high angle has been deduced beneath NE Colombia and NW Venezuela, and incorporated in models presented in Bezada et al. (2010), Masy et al. (2011) and van Benthem et al. (2013). This region coincides with the location of the Bucaramanga Nest (Bezada et al., 2010; Taboada et al., 2000) where brittle processes occur at 150–200 km depth, consistent with the existence of a cold upper mantle.

The greater abundance of positive time residuals in the southern portion (at latitudes south of 6°) in Figs. 7 and 8, with the greatest concentration of positive delays in the Pacific coast and the Western and Central Cordilleras, indicates the existence of a relatively slow seismic velocity in the upper mantle, in the region where Nazca subduction should be ongoing. Despite the very young age of the Nazca Plate (Tibaldi and Ferrari, 1992), its buoyancy should be enough to subduct.

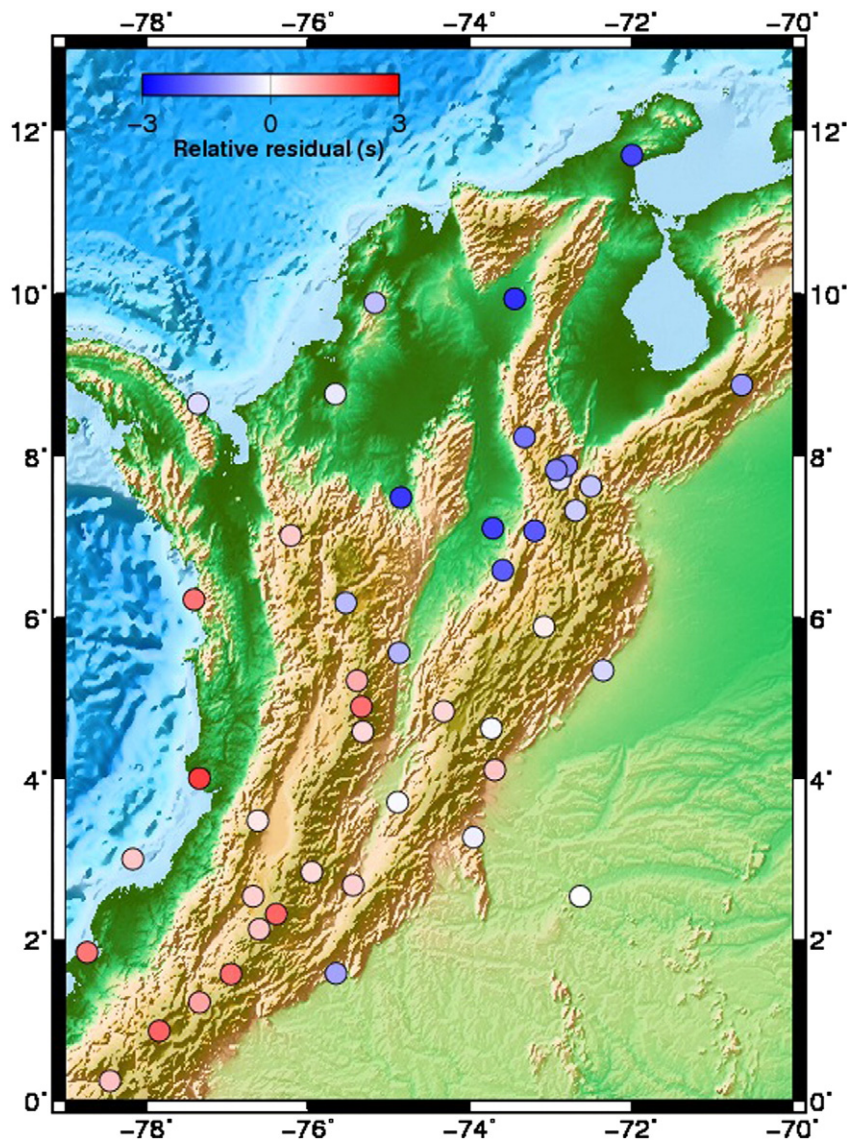


Fig. 8. Average differential teleseismic travel time residuals at each station relative to a regional mean. The effect of differential crustal thickness has been taken out. See text for explanation.

According to the relocated seismicity by Pedraza-García et al. (2007), the dip of Nazca subduction beneath western Colombia varies between 17° and 45°, at least for latitudes south of 5.5°N.

Nazca subduction beneath Colombia is associated with high heat flow values ( $>0.06 \text{ Wm}^{-2}$ ) in the Pacific Coast that indicate a relatively warm forearc (Pollack et al., 1993), according to the classification of Peacock (2003) for subduction zone forearcs. In terms of the age, the Nazca Plate should be comparable to the Philippine Sea Plate in southwestern Japan (Peacock, 2003; Peacock and Wang, 1999) but the seismicity suggests that for the most part, the subduction angle of the Nazca slab beneath Colombia is greater than the estimates for the Philippine Sea Plate. In any case, even for very young oceanic lithosphere, the plate should be negatively buoyant enough to subduct and to develop a mantle wedge (Cloos, 1993). Following the records of seismicity (Pedraza-García et al., 2007), lower crustal xenoliths (Weber et al., 2002) and the geochemistry of volcanic rocks (Kroonenberg et al., 1982), it is clear that subduction of the Nazca Plate beneath western Colombia, at least at several locations, is steep enough to generate such a wedge of asthenospheric material.

The boundary between the two subduction segments suggested by our observations (probably associated to Caribbean and Nazca plates) still remains uncertain: Figs. 7 and 8 suggest that such limit should

have a WNW-ESE direction, at latitude near 6°N, marking the transition between the regions of predominantly blue markers to the north and mostly red markers to the south. It is well known that the active current volcanism is limited to latitudes south of 5.5°N indicating that there may be a change in subduction style at that latitude, where Vargas and Mann (2013) hypothesize the presence of the “Caldas Tear”.

The existence of these two contrasting subduction segments in Northwestern South America should be linked to contrasts in the thermal structure and heat flow of different basins in the region. Heat flow estimates beneath basins in northernmost Colombia, at the Caribbean coastal plains, are between 33 and 38  $\text{mW/m}^2$  (Lopez and Ojeda, 2006), whereas for basins to the south (specifically between the Western and Central Cordilleras), flows are in the range from 40 to 69  $\text{mW/m}^2$  (Hamza et al., 2005). The thermal features of northernmost Colombia may be characteristic of a flat subduction regime, similar to the flat slab segment in the Central Andes of Argentina where the present heat flow estimations are between  $\sim 20$  and 30  $\text{mW/m}^2$  (Collo et al., 2011).

One way to interpret the path-integrated mantle and lithospheric velocity anomalies that are implied by our relative travel time anomalies is in light of their possible dynamic effect, by means of the associated density anomalies and/or the induced mantle flow.

Such sub-crustal anomalies will be reflected on the surface in terms of depressing or elevating topography beyond the level that would be expected from isostasy (e.g., [Lachenbruch and Morgan, 1990](#)). While we do not attempt to model these deep, dynamic topography effects here, we explore how the non-isostatic residual topography, inferred from the shallow layer structure, compares with our inferred delay time patterns.

Estimates of non-isostatic topography require a crustal thickness model, which was discussed earlier ([Fig. 4](#)). Using this model, we proceed with a standard analysis, with all details as in [Becker et al. \(2014\)](#), and first estimate the expected topography from Airy isostasy using constant crustal and lithospheric densities of  $2802 \text{ kg/m}^3$  (average from CRUST1 for the region) and  $3250 \text{ kg/m}^3$ , respectively. With a constant lithospheric thickness of 125 km, matching the average topography for the region requires a plausible asthenospheric density of  $3203 \text{ kg/m}^3$ . This estimate of expected topography from crustal thickness variations alone is then subtracted from the long-wavelength smoothed actual topography (to avoid flexural effects, using a  $\sim 300 \text{ km}$  width Gaussian kernel), and the resulting residual is shown in [Fig. 9a](#).

While absolute values and the average offset of topography are strongly dependent on parameter choices, the Airy residual estimate would imply anomalously high topography throughout much of Colombia, in what [Bird \(2003\)](#) identifies as the North Andes plate, with the exception of anomalously low topography centered on Maracaibo Lake. If we allow for crustal density variations (from CRUST1, as shown in [Fig. 4](#)), the residual topography plotted in [Fig. 9b](#) results. While density values are less well constrained than crustal thickness, the adjusted figure implies that some of the coastal topography anomalies may actually be due to crustal density variations. Several other features, such as the positive residual to the east of Bucaramanga, appear robust, however.

Besides crustal anomalies, we also strive to remove the effect of lithospheric thickness variations, at constant lithospheric density. In the absence of other, more detailed lithospheric thickness constraints, we use Voigt shear-wave velocity anomalies from the recent, radially anisotropic tomography model by [Auer et al. \(2014\)](#) which has fairly good resolution in the study area. We define the lithospheric depth as the vertical downward extent of velocity anomalies larger than 2%, limiting thicknesses to fall between 100 and 275 km. The resulting lithospheric thickness estimate implies relatively thin ( $\sim 100 \text{ km}$ ) lithosphere toward the west of a SSW-NNE oriented line, roughly in line with, and extending, the volcanic center trend ([Fig. 9](#)), and larger ( $\sim 175 \text{ km}$ ) thickness on the east of that line; the average thickness

is  $\sim 125 \text{ km}$ . As expected, when included in the residual topography estimate, these lithospheric thickness variations remove much of the western positive anomalies in our final estimate of residual topography ([Fig. 9c](#)).

Recognizing the uncertainties in such computations, we may then associate all remaining topographic anomalies in [Fig. 9c](#) with either lithospheric density variations, or a dynamics, mantle flow origin. Comparing the residual topography with our delay time anomalies, we find that small magnitude delay times (mostly negative) in central Colombia are associated with anomalously low topography, perhaps depressed by a cold mantle anomaly, or a probably Nazca slab-associated downwelling. In contrast, there is a pronounced positive topographic residual, stable for all estimates in [Fig. 9](#), just off the east of Bucaramanga, and also to the east where we have some indication of strongly negative delay times.

The tectonic origin of the residual topography, and the link to deep structure and dynamics, remain to be further explored based on seismic tomography. However, our results are consistent with a fairly coherent, roughly SSW-NNE oriented slab structure underneath Colombia, presumably associated with subduction of both Nazca and Caribbean plates. On top of this, there is some indication of a hot anomaly, or an upwelling, off the slab east of Bucaramanga, perhaps associated with flow through a slab gap, or induced by slab-associated return flow (cf. [Faccenna et al., 2010](#)).

Two cartoons with our preferred model for Caribbean and Nazca subduction are presented in [Fig. 10](#). In the northernmost Colombia, we propose a scenario of thin crust, cold lithosphere and flat subduction. In this region, earthquakes are relatively scarce, probably related with the absence of very contrasting GPS vectors between the Caribbean Sea and the Colombian coastal plains ([Trenkamp et al., 2002](#)); the mean earthquake depth in the northern Caribbean plains is  $\sim 37 \text{ km}$  according to the ISC Catalog (EHB Bulletin), where we suspect that the subducting plate has a shallow angle. This angle should steepen near the location of the Bucaramanga nest. This is suggested by the results presented in [Figs. 7 and 8](#), where the location of this nest seems to be related with the northern subduction segment that shows negative residuals. [Prieto et al. \(2012\)](#) proposed a mechanism for their origin that consists of a thermal shear instability, with the earthquakes being generated along subparallel faults within a subducted slab. [Zarifi et al. \(2007\)](#) establish that it is difficult to associate the seismicity of the Bucaramanga Nest either with a subducted portion of the Caribbean Plate, with the Nazca Plate or with a collision of both. The association of this nest with the northern segment suggests that it is generated within a subducted Caribbean slab. The lithospheric thicknesses related

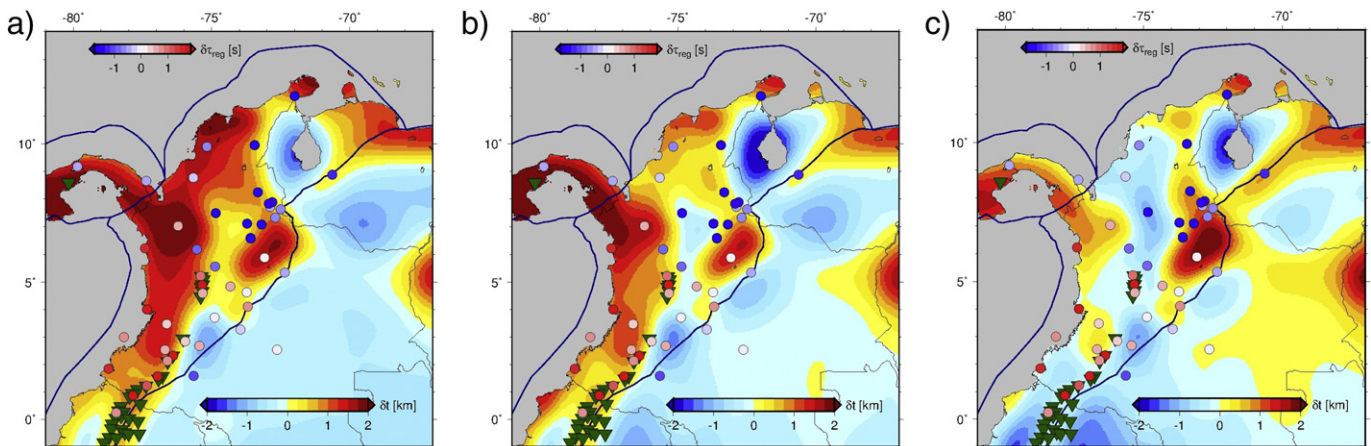


**Fig. 9.** Residual (anomalous, non-isostatic) topography and relative delay times,  $dt$ , relative to station HEL. Plate boundaries are from [Bird \(2003\)](#), and green inverted triangles show recent volcanism from [Siebert and Simkin \(2002\)](#). a) Residual topography after removal of a constant density crustal layer with thickness as in [Fig. 4](#). b) After removal of a variable density crustal layer with densities as in [Fig. 4](#). c) After removal of a variable density crustal layer, and correcting for lithospheric thickness variations as inferred from the SAVANI tomography model by [Auer et al. \(2014\)](#), see the text for details.

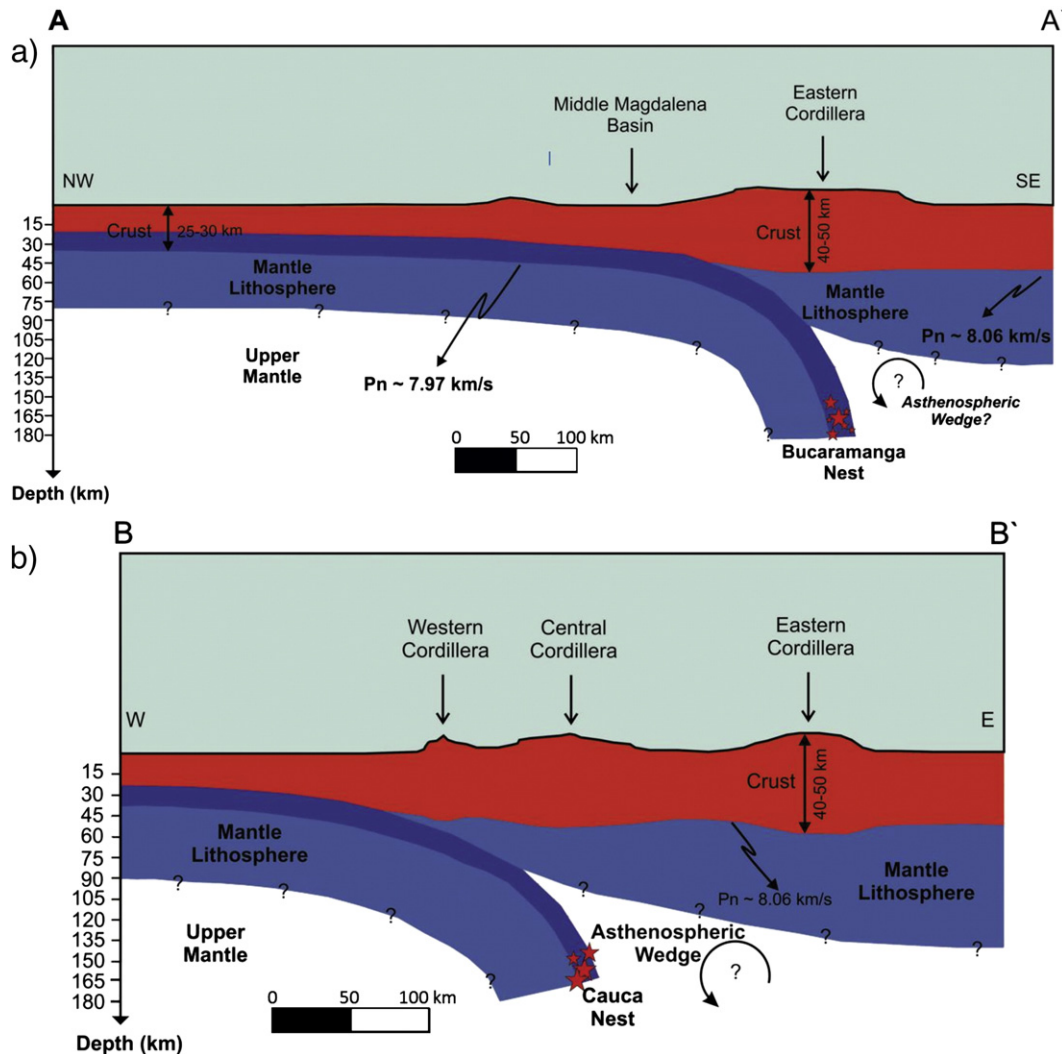


**Fig. 10.** Schematic section of (a) Caribbean subduction beneath Northwestern Colombia and (b) Nazca subduction beneath Western Colombia along sections A-A' and B-B' respectively from Fig. 1.

with the two segments suggested in Figs. 7 and 8, and the possible presence of an asthenospheric wedge beneath the Eastern Cordillera, remain unclear. In Fig. 10 we illustrate Nazca subduction beneath western Colombia after tomographic images from Van der Hilst and Mann (1994) and models from Corredor (2003) and Cortes and Angelier (2005).

## 6. Summary and conclusions

The spatial distribution of relative teleseismic travel time residuals, after removing the effects of differential crustal thickness, is consistent with the presence of at least two subduction segments beneath the northwesternmost Andes of South America. Residuals in the northernmost Colombia have a relatively small magnitude, with the presence of positive and negative delays, and a Pn speed of 7.97 km/s. Strongly negative residuals concentrate beneath the northern Eastern Cordillera (which includes the Bucaramanga nest), the vicinities of the Perija and San Lucas ranges, and the Merida Andes; just to the east of Bucaramanga there is a strong signal of positive residual topography; values of Pn speed beneath the Northern Eastern Cordillera are ~8.07 km/s.

These features favor a model with an initially flat subduction beneath the Caribbean coastal plains, where the crust is relatively thin (~30 km); to the southeast, the crust should become thicker,

and the upper mantle should be colder. At around the location of Bucaramanga, there may be a steepening of the slab; the positive residual topography just to the east of this area may be related to a hot anomaly, representing upwelling as a consequence of slab-associated asthenospheric return-flow.

In the Central and Southern Andes of Colombia, there are alternating positive and negative teleseismic travel time delays, with the positive residuals concentrating in the western Andes and the Pacific coast. The residuals decrease to the east, where residual topography is negative, which perhaps represents a Nazca slab-related downwelling. This is consistent with the well-known presence of an asthenospheric wedge beneath the Central and Southern Andes of Colombia, where active volcanoes are located.

## Appendix A. Supplementary data

Supplementary data to this article can be found online at <http://dx.doi.org/10.1016/j.tecto.2014.09.006>.

## References

- Amini, S., Shomali, Z.H., Koyi, H., Roberts, R.G., 2012. Tomographic upper-mantle velocity structure beneath the Iranian Plateau. *Tectonophysics* 554, 42–49.

- Assumpção, M., Feng, M., Tassara, A., Julià, J., 2013. Models of crustal thickness for South America from seismic refraction, receiver functions and surface wave tomography. *Tectonophysics* 609, 82–96.
- Auer, L., Boschi, L., Becker, T.W., Nissen-Meyer, T., Giardini, D., 2014. Savani: A variable resolution whole-mantle model of anisotropic shear velocity variations based on multiple data sets. *J. Geophys. Res. Solid Earth* 119 (4), 3006–3034.
- Becker, T.W., et al., 2014. Static and dynamic support of western U.S. topography. *Earth Planet. Sci. Lett.* 402, 234–246.
- Bezada, M.J., Levander, A., Schmandt, B., 2010. Subduction in the Southern Caribbean: images from finite-frequency P-wave tomography. *J. Geophys. Res.* 115 (B12).
- Bird, P., 2003. An updated digital model of plate boundaries. *Geochem. Geophys. Geosyst.* 4 (3).
- Bonini, W.E., 1984. Magnetic provinces in western Venezuela. *Mem. Geol. Soc. Am.* 162, 161–174.
- Calvache, M.L., Cortés, G.P., Williams, S.N., 1997. Stratigraphy and chronology of the Galeras volcanic complex, Colombia. *J. Volcanol. Geotherm. Res.* 77 (1–4), 2–19.
- Cardona, A., et al., 2012. From arc–continent collision to continuous convergence, clues from Paleogene conglomerates along the southern Caribbean–South America plate boundary. *Tectonophysics* 580, 58–87.
- Ceron, J.F., Kellogg, J.N., Ojeda, G.Y., 2007. Basement configuration of the northwestern South America–Caribbean margin from recent geophysical data. *CT&F – Cienc., Tecnol. Futuro* 3, 25–49.
- Christensen, N.L., Mooney, W.D., 1995. Seismic velocity structure and composition of the continental crust: a global view. *J. Geophys. Res.* 100 (B7), 9761–9788.
- Cloos, M., 1993. Lithospheric buoyancy and collisional orogenesis: subduction of oceanic plateaus, continental margins, island arcs, spreading ridges, and seamounts. *Geol. Soc. Am.* 105 (6), 715–737.
- Collo, G., et al., 2011. Clay mineralogy and thermal history of the Neogene Vinchina Basin, central Andes of Argentina: analysis of factors controlling the heating conditions. *Tectonics* 30 (4).
- Corredor, F., 2003. Seismic strain rates and distributed continental deformation in the northern Andes and three-dimensional seismotectonics of northwestern South America. *Tectonophysics* 372, 147–166.
- Cortés, M., Angelier, J., 2005. Current states of stress in the northern Andes as indicated by focal mechanisms of earthquakes. *Tectonophysics* 403, 29–58.
- Crotwell, H.P., Owens, T.J., Ritsema, J., 1999. The TauP Toolkit: flexible seismic travel-time and raypath utilities. *Seismol. Res. Lett.* 70 (2), 154–160.
- Ding, X.-Y., Grand, S.P., 1994. Seismic structure of the deep Kurile Subduction Zone. *J. Geophys. Res. Solid Earth* (1978–2012) 99 (B12), 23767–23786.
- Faccenna, C., et al., 2010. Subduction-triggered magmatic pulses: a new class of plumes? *Earth Planet. Sci. Lett.* 299 (1), 54–68.
- Flinch, J., 2003. Structural evolution of the Sinu-Lower Magdalena area (Northern Colombia). In: Bartolini, C., Buffer, R., Blickwede, J. (Eds.), *The Circum-Gulf of Mexico and the Caribbean: hydrocarbon habitats, basin formation, and plate tectonics*. AAPG Memoir 79, pp. 141–143.
- Franco, E., et al., 2002. Sismicidad registrada por la Red Sismológica Nacional de Colombia durante el tiempo de operación: junio de 1993 hasta agosto de 2002. 1° Simposio Colombiano de Sismología. Bogotá, 2002. 1° Simposio Colombiano de Sismología.
- Gutscher, M.-A., Spakman, W., Bijwaard, H., Engdahl, E.R., 2000. Geodynamics of flat subduction: seismicity and tomographic constraints from the Andean margin. *Tectonics* 19 (5), 814–833.
- Hanza, V.M., Silva Dias, F.J.S., Gomes, A.J.L., Delgadillo-Terceros, Z.G., 2005. Numerical and functional representations of regional heat flow in South America. *Phys. Earth Planet. Inter.* 152, 223–256.
- Hearn, T.M., Ni, J.F., 1994. Pn velocities beneath continental collision zones: the Turkish–Iranian Plateau. *Geophys. J. Int.* 117 (2), 273–283.
- Hearn, T.M., Rosca, A.C., Fehler, M.C., 1994. Pn tomography beneath the Southern Great Basin. *Geophys. Res. Lett.* 21 (20), 2187–2190.
- Hirn, A., Sapin, M., 1984. The Himalayan zone of crustal interaction: suggestions from explosion seismology. *Ann. Geophys.* 2 (2), 123–130.
- Hoernle, K., et al., 2002. Missing history (16–71 Ma) of the Galápagos hotspot: implications for the tectonic and biological evolution of the Americas. *Geology* 30 (9), 795–798.
- Kellogg, J.N., Vega, V., 1995. Tectonic development of Panama, Costa Rica, and the Colombian Andes: constraints from Global Positioning System geodetic studies and gravity. In: Mann, P. (Ed.), *Geologic and Tectonic Development of the Caribbean Plate Boundary in Southern Central America: Special Paper 295*. Boulder, Colorado: Geological Society of America Special Paper 295, pp. 75–90.
- Kennan, L., Pindell, J., 2009. Dextral shear, terrane accretion and basin formation in the Northern Andes: best explained by interaction with a Pacific-derived Caribbean Plate. *Geol. Soc. Lond. Spec. Publ.* 328, 487–531.
- Kennett, B.L.N., Engdahl, E.R., 1991. Traveltimes for global earthquake location and phase identification. *Geophys. J. Int.* 105, 429–465.
- Kerr, A.C., Tarney, J., 2005. Tectonic evolution of the Caribbean and northwestern South America: the case of two late Cretaceous oceanic plateaus. *Geology* 33 (4), 269–272.
- Kroonenberg, S.B., Pichler, H., Diederix, H., 1982. Cenozoic alkalibasaltic to ultrabasic volcanism in the Uppermost Magdalena Valley, South-central Huila Department, Colombia. *Geologia Norandina* (Bogotá) 5, 19–26.
- Lachenbruch, A.H., Morgan, P., 1990. Continental extension, magmatism and elevation: formal relations and rules of thumb. *Tectonophysics* 174 (1), 39–62.
- Lara, M., et al., 2013. Middle Miocene near trench volcanism in northern Colombia: a record of slab tearing due to the simultaneous subduction of the Caribbean Plate under South and Central America? *J. S. Am. Earth Sci.* 45, 24–41.
- Laske, G., Masters, G., Ma, Z., Pasyanos, M., 2013. Update on CRUST1.0—a 1-degree global model of Earth's crust. EGU General Assembly.
- Lonsdale, P., 2005. Creation of the Cocos and Nazca plates by fission of the Farallon plate. *Tectonophysics* 404 (3–4), 237–264.
- Lopez, C., Ojeda, G.Y., 2006. Heat flow in the Colombian Caribbean from the Bottom Simulating Reflector (BSR). *CT&F – Cienc., Tecnol. Futuro* 3 (2), 29–39.
- Lu, Y., Ni, S., Liu, B., Sun, Y., 2011. Pn tomographic velocity and anisotropy beneath the Tibetan Plateau and the adjacent regions. *Earth Planets Space* 63, 1169–1173.
- Macellari, C.E., 1995. Cenozoic sedimentation and tectonics of the southwestern Caribbean pull-apart basin, Venezuela and Colombia. In: Tankard, A.J., Suárez, R., Welsink, H.J. (Eds.), *Petroleum basins of South America*. AAPG Memoir 62, pp. 757–780.
- Marriner, G., Millward, D., 1984. The petrology and geochemistry of Cretaceous to Recent volcanism in Colombia; the magmatic history of an accretionary plate margin. *J. Geol. Soc. Lond.* 141 (3), 473–486.
- Masy, J., Niu, F., Levander, A., Schmitz, M., 2011. Mantle flow beneath northwestern Venezuela: seismic evidence for a deep origin of the Mérida Andes. *Earth Planet. Sci. Lett.* 305 (3–4), 396–404.
- Mauffret, A., Leroy, S., 1997. Seismic stratigraphy and structure of the Caribbean igneous province. *Tectonophysics* 283, 61–104.
- Maya, M., 1992. Catálogo de dataciones isotópicas en Colombia. *Bol. Geol. – Ingeominas* 32, 127–188.
- Meschede, M., Barckhausen, U., 2000. Plate tectonic evolution of the Cocos–Nazca spreading center. In: Silver, E.A., Kimura, G., Shipley, T.H. (Eds.), *Proceedings of the Ocean Drilling Program, Scientific Results vol. 170*. Federal Institute for Geosciences and Natural Resources, Hannover, Germany, pp. 1–10.
- Monsalve, G., Sheehan, A., Rowe, C., Rajaure, S., 2008. Seismic structure of the crust and the upper mantle beneath the Himalayas: evidence for eclogitization of lower crustal rocks in the Indian Plate. *J. Geophys. Res.* 113 (B08315).
- Monsalve, H., Pacheco, J.F., Vargas, C.A., Morales, Y.A., 2013. Crustal velocity structure beneath the western Andes of Colombia using receiver-function inversion. *J. S. Am. Earth Sci.* 48, 106–122.
- Montes, C., et al., 2010. Clockwise rotation of the Santa Marta massif and simultaneous Paleogene to Neogene deformation of the Plato–San Jorge and Cesar–Ranchería basins. *J. S. Am. Earth Sci.* 29, 832–848.
- Müller, R.D., Sdrolias, M., Gaina, C., Roest, W.R., 2008. Age, spreading rates, and spreading asymmetry of the world's ocean crust. *Geochem. Geophys. Geosyst.* 9 (4), 1–19.
- Ojeda, A., Havskov, J., 2001. Crustal structure and local seismicity in Colombia. *J. Seismol.* 5, 575–593.
- Peacock, S.M., 2003. Thermal structure and metamorphic evolution of subducting slabs. In: Eiler, J. (Ed.), *Inside the Subduction Factory*. American Geophysical Union, Washington D.C.
- Peacock, S.M., Wang, K., 1999. Seismic consequences of warm versus cool subduction metamorphism: examples from Southwest and Northeast Japan. *Science* 286 (5441), 937–939.
- Pedraza-García, P., Vargas-Jimenez, C.A., Monsalve, J.H., 2007. Geometric model of the Nazca Plate subduction in Southwest Colombia. *Earth Sci. Res. J.* 11 (2), 117–130.
- Pennington, W.D., 1981. Subduction of the Eastern Panama Basin and Seismotectonics of Northwestern South America. *J. Geophys. Res.* 86 (B11), 10753–10770.
- Pollack, H.N., Hurter, S.J., Johnson, J.R., 1993. Heat flow from the earth's interior: analysis of the global data set. *Rev. Geophys.* 31 (3), 267–280.
- Poveda, E., Monsalve, G., Vargas-Jimenez, C.A., 2013. Receiver function study of the crustal structure beneath Northern Andes. AGU Spring Meeting. Abstract T23A-02 presented at 2013 Spring Meeting, AGU, Cancun, Mexico, 14–17 May, 2013.
- Poveda, H.E., Monsalve, G., Vargas, C.A., 2014. Receiver functions and crustal structure of the northwestern Andean Region, Colombia. *J. Geophys. Res.* (under review).
- Prieto, G.A., et al., 2012. Earthquake nests as natural laboratories for the study of intermediate-depth earthquake mechanics. *Tectonophysics* 570–571, 42–56 (Review Article).
- Shih, X.R., Meyer, R.P., Schneider, J.F., 1991. Seismic anisotropy above a subducting plate. *Geology* 19, 807–810.
- Siebert, L., Simkin, T., 2002. *Volcanoes of the world: an illustrated catalog of Holocene volcanoes and their eruptions*. Global Volcanism Program Digital Inf. Ser., GVP 3.
- Stern, T., et al., 2010. Crust–mantle structure of the central North Island, New Zealand, based on seismological observations. *J. Volcanol. Geotherm. Res.* 190, 58–74.
- Taboada, A., et al., 2000. Geodynamics of the northern Andes: subductions and intracontinental deformation (Colombia). *Tectonics* 19 (5), 787–813.
- Tibaldi, A., Ferrari, L., 1992. Latest Pleistocene–Holocene tectonics of the Ecuadorian Andes. *Tectonophysics* 205, 109–125.
- Toto, E., Kellogg, J., 1992. Structure of the Sinu-San Jacinto fold belt—An active accretionary prism in northern Colombia. *J. S. Am. Earth Sci.* 5 (1), 211–222.
- Trenkamp, R., Kellogg, J.N., Mora, H.P., Freymueller, J.T., 2002. Wide plate margin deformation, southern Central America and northwest South America, CASA GPS observations. *J. S. Am. Earth Sci.* 15, 157–171.
- van Benthem, S., Govers, R., Spakman, W., Wortel, R., 2013. Tectonic evolution and mantle structure of the Caribbean. *J. Geophys. Res. Solid Earth* 118 (6), 3019–3036.
- Van der Hilst, R., Mann, P., 1994. Tectonic implication of tomographic images of subducted lithosphere beneath northwestern South America. *Geology* 22, 451–454.
- vanHunen, J., van der Berg, A.P., Vlaar, N.J., 2002. On the role of subducting oceanic plateaus in the development of shallow flat subduction. *Tectonophysics* 352 (3–4), 317–333.
- Vargas, C.A., Mann, P., 2013. Tearing and breaking off of subducted slabs as the result of collision of the Panama Arc-Indenter with Northwestern South America. *Bull. Seismol. Soc. Am.* 103 (3), 2025–2046.
- Wéber, Z., 2002. Imaging Pn velocities beneath the Pannonian basin. *Phys. Earth Planet. Inter.* 129 (3–4), 283–300.
- Weber, M.B.I., Tarney, J., Kempton, P.D., Kent, R.W., 2002. Crustal make-up of the northern Andes: evidence based on deep crustal xenolith suites, Mercaderes, SW Colombia. *Tectonophysics* 345 (1–4), 49–82.
- Zarifi, Z., Havskov, J., Hanyga, A., 2007. An insight into the Bucaramanga nest. *Tectonophysics* 443 (1–2), 93–105.
- Zhou, R., Grand, S.P., Tajima, F., Ding, X.-Y., 1996. High velocity zone beneath the southern Tibetan plateau from P-wave differential travel-time data. *Geophys. Res. Lett.* 23 (1), 25–28.